

Temperature Effect on THz Quantum Cascade Lasers

Aida Gholami¹, Hassan Rasooly²

¹Department of Electrical Engineering, Ahar Branch, Islamic Azad University, Ahar, Iran.
Email: aida_gholami1986@yahoo.com (corresponding author)

¹Department of Electrical Engineering, Tabriz Branch, Islamic Azad University, Tabriz, Iran.
Email: h_rasooly_s@yahoo.com

ABSTRACT

A simple semi-phenomenological model, which accurately predicts the dependence of threshold current for temperature of Resonant-phonon three well quantum cascade laser based on vertical transitions is offered. We found that, the longitude optical phonon scattering of thermally excited electrons is the most important limiting factor for thermal performance of high frequency THz QCLs. In low frequency region, parasitic current increases the threshold current. Based on our model the use of materials with higher longitude optical phonon energy such as InGaAs/GaAsSb and decreasing the lower laser level lifetime can increase the maximum performance temperature. Our observations may can be used to understand the notion of the effects of thermal electrons on reduction of laser performance.

KEYWORDS: Quantum cascade lasers, longitude optical phonon, intersubband transitions, Parasitic current.

1. INTRODUCTION

Quantum cascade lasers (QCLs) are semiconductor lasers based on intersubband transitions in multi quantum well heterostructures, which rely on epitaxial growth techniques [1]. They are very versatile mid-infrared sources for the realization of Ultrasensitive and selective sensors for spectroscopic applications in the fields of environmental monitoring, industrial processes, security and military [2].

Terahertz quantum-cascade lasers (THz QCLs) now provide spectral coverage from $\nu = 1.2 - 5$ THz with optical pomilliwatt in the tens of milli-Watt range, and are poised to become one of the most important types

of terahertz radiation source [3]

So far among all existing designs, the three-well resonant phonon based THz QCLs, originally proposed by Luo et al. [4], have demonstrated the best temperature performance [5]. The major effect of temperature rising on laser performance as follows:

Low temperature performance of THz QCLs is a major problem. The temperature affects inter and intrasubband lifetimes by the Bose-Einstein factor. Although this is fortunately a weak coupling, the effective upper state lifetime decreases with increasing temperature affecting inversely the threshold current density. The atomic-like joint density of states is beneficially

since this will avoid direct temperature broadening of the linewidth. However, the linewidth is collision broadened by the ultra-short inter and intrasubband lifetimes. Linewidth broadening has a detrimental effect on the gain cross section and increases the non-resonant intersubband losses; both reduce the threshold current density. Furthermore, the temperature increases the backfilling and consequently the larger non-resonant losses will increase the threshold current density.

Improving the maximum operating temperatures of THz

QCLs still further is highly attractive for a range of technological applications. This is made inherently more difficult in the THz frequency range than in the mid-infrared (MIR) due to the smaller photon energy (typically less than 20 meV). At higher lattice temperatures (and, hence, higher electron temperatures), it becomes more difficult to achieve selective injection and depopulation of the upper and lower laser levels. Additionally, since the photon energy is less than the LO phonon energy (36 meV in GaAs) in the THz frequency range, at sufficiently high electron temperatures, thermally activated LO phonon .The maximum operating temperature demonstrated to date, without a magnetic field, is 186 K [6] for pulsed operation and 117 K for CW operation [7]. With an applied magnetic field of 20–30 T, THz QCLs can operate at higher temperatures, with $T_{\max} \approx 225$ K demonstrated for 3-THz devices [8].

Several theoretical models have been employed to understand the details of charge transport and optical gain within THz QCLs, based on various approaches such as density matrix (DM) [9], non-

equilibrium Green function [10], and Monte Carlo (MC) techniques [11]. We are going to provide a model to explain the decrease of gain at higher temperatures. We present a simple semi-phenomenological model, which accurately predicts the threshold current dependence for 3QW QCL design with a vertical (the lower and upper laser levels located in the same well) lasing transition. This study may lead to a better understanding of the notion of the effects of thermal electrons on reduction of laser performance.

2. THEORETICAL MODEL

The electron can lose its energy by colliding with other electrons, emitting photons, emitting optical and acoustical phonons, and by interacting with interface surface and impurities. It seems that, the LO phonon scattering of thermal electrons is the main factor of low performance. Accordingly, this is because of the fact that when the temperature of electrons is increased, instead of photon emission and leaving the upper level they emit LO phonons.

The population inversion in a two level system is described by the following equation

$$n_2 - n_1 = \frac{J_{\text{eff}}(\tau_{21} - \tau_1)}{e} \quad (1)$$

τ_1 is the electron lifetime in the lower laser level (in our case, it is determined by resonant tunneling into the injector and subsequent optical phonon scattering), τ_{21} is the electron scattering time from state 2 to state 1 (which is determined by optical phonon scattering of thermal electrons in state 2 and $J_{\text{eff}} = J - J_{\text{par}}$). The threshold current for this laser is given as follows:

$$J_{th} = J_{par} + \alpha_{tot} \cdot \left(\frac{\epsilon_0 h c n_{eff}}{4\pi e} \right) \cdot \left(\frac{\delta\nu}{\nu_0} \right) \cdot \left(\frac{L_{per}}{|z|^2} \right) \frac{1}{\tau_{21} - \tau_1} \quad (2)$$

Where α_{tot} are the total optical losses in the laser, n_{eff} is the modal effective index, z is the optical dipole moment for the laser transition, $\delta\nu$ is the full-width at half-maximum (FWHM) of the laser transition at frequency ν_0 , and L_{per} is the length of one period. Equation (2) can be rewritten in typical units used in experiments as

$$J_{th} = J_{par} + 31.5 \alpha_{tot} \left(\frac{\delta\nu}{\nu_0} \right) \left(\frac{L_{per}}{|z|^2} \right) \frac{1}{\tau_{21} - \tau_1} \quad (3)$$

In the above equation, length, time and total optical losses are written in nanometer, picoseconds and cm^{-1} units.

When the energy separation between the upper and lower laser levels is less than the LO-phonon energy, and the electron density in state 2 is low so that the Fermi energy is much smaller than $K_B T$, we can approximate the electron scattering time from state 2 to state 1 (τ_{21}) as follows:

$$\frac{1}{\tau_{21}} = \frac{1}{\tau_{21,0}} + \frac{1}{\tau_{21,hot}} e^{-\frac{h\nu - E_{LO}}{K_B T_e}} \quad (4)$$

Where, $\tau_{21,0}$ is the upper level lifetime at 0K, and $\tau_{21,hot}$ is the lifetime of electrons in level 2 which can emit optical phonons and relax to level 1. In order to obtain the above equation we used the assumption $\tau_{21,0} > \tau_{21,hot}$.

Using Eq. (4) and (3) the temperature dependence of threshold current obtained as

$$J_{th} = J_{par} + \frac{B}{\tau_1} \left(\frac{1}{1 - \frac{\tau_1}{\tau_{21,hot}} e^{-\frac{h\nu - E_{LO}}{K_B T_e}}} - 1 \right) \quad (5)$$

Where $B = 31.5 \alpha_{tot} \left(\frac{\delta\nu}{\nu_0} \right) \left(\frac{L_{per}}{|z|^2} \right)$. Experimental

data for threshold and parasitic current is obtained in [12]. The frequency values of these lasers are 2.3, 2.7, 3.1, 3.5 and 3.8 THz. Fig.1 shows the experimental values of threshold current for some THz QCLs with different frequencies which are obtained as a heat sink temperature.

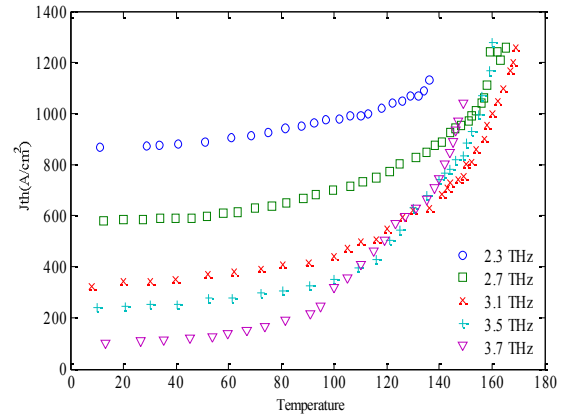


Fig. 1. The threshold current obtained in various heat sink temperatures for some THz QCLs with different frequencies [12].

We can obtain the values of B/τ_1 and $\tau_1/\tau_{21,hot}$ through fitting the above equation with experimental data and compare them with theoretical values obtained in [13, 14].

3. RESULT AND DISCUSSION

3.1. Parasitic current

Parasitic current appears when electrons go through some unwanted channel. This current appears in all bias voltages; however, in this section we focus on parasitic current, which occurs due to electron tunneling from the active region. In

fact, this occurs when the energy of the electron rises to a specific value. We show this current in Fig.2 schematically. When the energy of the electron reaches to this point, the instability appears in the current-voltage graph of the laser. At this point, the second derivative of the current-voltage curve vanishes.

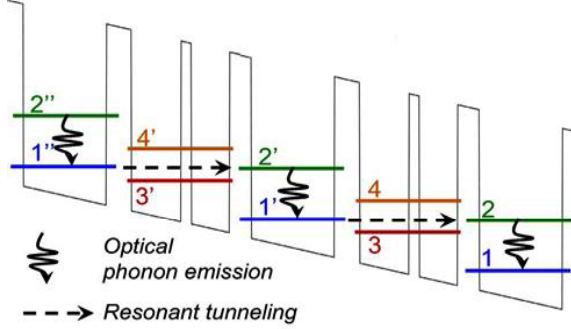


Fig.2. Level alignment and electron tunneling through active region in parasitic bias [12].

Assuming coherent electron tunneling from level 1 to 2, one can utilize the tight-binding model [15] and derive the parasitic current. Taking the system with weak coupling, the current density reads:

$$J_{par} = \frac{eN}{2} \frac{(\Delta_{12}/\hbar)^2 \tau_{\parallel}}{(1 + (\Delta_{12}/\hbar)^2 \tau_{\parallel} \tau)} \quad (6)$$

Where Δ_{12} is the anticrossing energy between levels 1 and 2 at the parasitic alignment, N is the doping density, τ is the phonon emission time in the upper injector state (state 2), and $\frac{1}{\tau_{\parallel}} = \frac{1}{2\tau} + \frac{1}{T_2^*}$, where T_2^* is a pure dephasing time.

If the Schrödinger-Poisson method is used for calculating anticrossing energy, the following values can be resulted in parasitic current, which are in a good agreement with the experimental data given in [12].

Table 1. The calculated and experimental value of parasitic current.

ν (THz)	2.3	2.7	3.1	3.5	3.8
Δ_{12}	1.08	0.94	0.79	0.74	0.68
$J_{par(cal)}$	1025	879	701	640	566
$J_{par(exp)}$	991 ± 54	827 ± 53	623 ± 70	508 ± 70	462 ± 70

As it can be seen, parasitic current, have higher values in lower frequencies and increase the threshold current.

3.2. LO PHONON SCATTERING

If the temperature of electron equals with heat sink, we get the best fit with $\frac{B}{\tau_1} \approx 305.23$, and $\frac{\tau_1}{\tau_{21,hot}} \approx 3.19$; however,

there is a little difference with theoretical ($\frac{B}{\tau_1} \approx 144$, $\frac{\tau_1}{\tau_{21,hot}} \approx 2.7$) value obtained for

this parameters in [13,14].

This is due to the equality assumption of electron temperature with heat sink temperature. In fact, this assumption is not valid, and there is a temperature difference of the range 50 to 100 between electron and lattice.

Fig.3 shows the results abstained from fitting equation (5) with experimental data. A temperature difference of 50 degrees between the electron and the heat sink was considered. As it can be seen, there is a good accordance between represented model and experimental data. The values of

parameters, $\frac{\tau_1}{\tau_{21,hot}} \approx 2.832$ are in good

agreement with the theoretical value of this parameter.

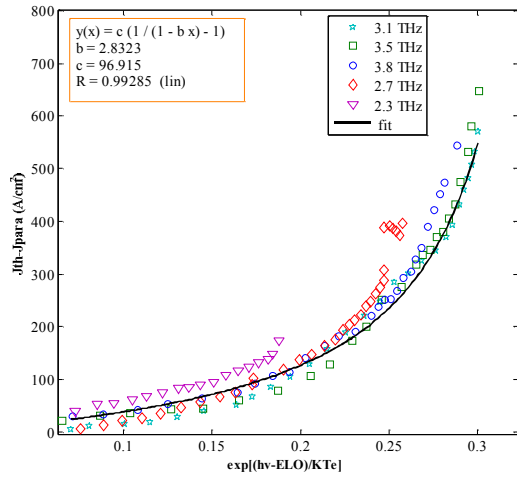


Fig. 3. The experimental value of $J_{th} - J_{par}$ as a function of $\exp[(hv - E_{LO}) / kT_e]$

Using equation (4), the maximum performance temperature can be given as

$$T_{max} \approx \frac{E_{LO} - hv}{K_B \ln\left(\frac{\tau_1}{\tau_{21,hot}}\right)} \quad (7)$$

This relation for 2 THz laser results in $T_{max} \approx 250$ and for 4 THz laser results in $T_{max} \approx 182$. We see that this model gives an upper temperature bound for vertical 3 well QCLs. In order to improve the temporal performance of these lasers we can offer various solutions. In the first stage, we can reduce parasitic current. According to (6), the less anticrossing energy is, the less this current will be. In the second stage, we can use materials with lower E_{LO} such as *InGaAs / GaAsSb*.

In order to obtain the equation (7) we have used the assumption $\tau_{21,0} > \tau_{21,hot}$. Now, if we neglect this assumption the maximum performance temperature will be

$$T_{max} \approx \frac{-E_{LO} + hv}{K_B \ln\left[\left(1 - \frac{\tau_1}{\tau_{210}}\right) \frac{\tau_{21,hot}}{\tau_1}\right]} \quad (8)$$

In Fig. 4 the effect of a lower laser lifetime on maximum temperature has been shown.

We see that a little variation in these parameters can increase T_{max} drastically.

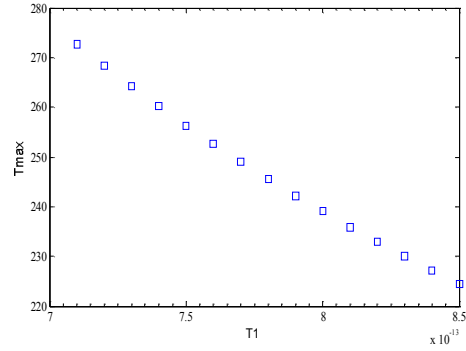


Fig. 4. Variation of maximum temperature versus lifetime of lower level in laser.

The LO phonon emission rate reduces drastically in diagonal transition. Hence, in this section we apply this model to a THz QCLs with the vertical transition with performance temperature of 186 k. the performance frequency of this laser is 3.9 THz and optical dipole moment is 5.9.

In the previous section we have seen that according to the definition, B was proportional to z^{-2} ; however, in this section we offer a new quantity $u = \left[\frac{z_{veric}}{z_{diag}}\right]^2$, () and

therefore, B must be replaced by Bu. The phonon emission rate of thermal electrons in diagonal transitions is proportional to z^2 [16]. Thus, in previous model we replace $\frac{\tau_1}{\tau_{21,hot}}$ with $\frac{\tau_1}{\tau_{21,hot}} \cdot u^{-1}$. τ_1 and L_{per} are same for both lasers. The data obtained with this model are compared with data given in [17]. As it can be found from the plot, there is a reasonable and satisfactory accordance between experimental and

theoretical data based on the proposed model. According to this model, the

maximum performance temperature can be more than 700 k.

Also the maximum performance according to this model is very high; but, other factors as low z increase the threshold current of these lasers.

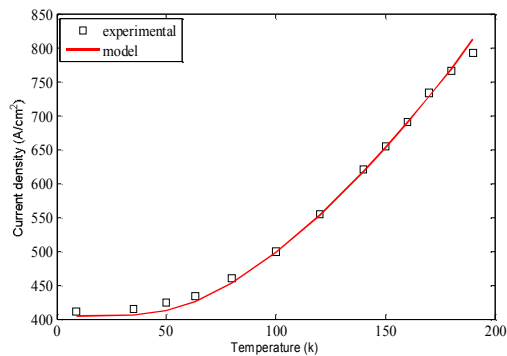


Fig.5. The experimental and calculated threshold current for vertical THz QCL.

5. CONCLUSIONS

Therefore, it can be concluded that for three well THz QCLs designed based on vertical transmissions, the maximum performance temperature is limited by LO phonon scattering of thermally excited electrons. We can improve the maximum performance temperature using materials with higher E_{LO} and decreasing the electron lifetime in the lower laser level with lifetime engineering.

In Diagonal transitions, LO-phonon scattering significantly reduces, so using this kind of transitions can be a useful alternative for constricting a THz QCL at room temperature.

REFERENCES

- [1] J. Faist, F. Capasso, C. Sirtori, D. L. Sivco, A. L. Hutchinson, S. N. G. Chu, and A. Y. Cho, *Electron. Lett.*, vol. 29, p. 2230, 1993.
- [2] A. Kosterev *et al.*, "Application of quantum cascade lasers to trace gas analysis", *Appl. Phys.*, Vol. 90, pp. 165, 2008.
- [3] B. S. Williams, "Terahertz quantum-cascade lasers," *Nature Photonics*, vol. 1, p. 517, 2007.
- [4] H. Luo, S. R. Laframboise, Z. R. Wasilewski, and H. C. Liu, "Terahertz quantum cascade lasers based on a three-well active module," *Appl. Phys. Lett.*, vol. 90, 041112, 2007.
- [5] S. Kumar, Q. Hu, and J. L. Reno, "186 K operation of terahertz quantum cascade lasers based on a diagonal design," *Appl. Phys. Lett.* Vol. 94, pp. 131105, 2009.
- [6] S. Kumar, Q. Hu, and J. L. Reno, "186 K operation of terahertz quantum-cascade lasers based on a diagonal design," *Appl. Phys. Lett.*, vol. 94, 2009.
- [7] B. S. Williams, S. Kumar, Q. Hu, and J. L. Reno, "Operation of terahertz quantum-cascade lasers at 164 K in pulsed mode and at 117 K incontinuous-wave mode," *Opt. Exp.*, vol. 13, pp. 3331–3339, 2005.
- [8] A. Wade, G. Fedorov, D. Smirnov, S. Kumar, B. S. Williams, Q. Hu, and J. L. Reno, "Magnetic-field-assisted terahertz quantum cascade laser operating up to 225 K," *Nature Photon*, vol. 3, pp. 41–45, 2009
- [9] R. Terrazi and J. Faist, "A density matrix model of transport and radiation in quantum cascade lasers," *New J. Phys.* Vol, 12, pp, 033045, 2010.
- [10] S. C. Lee and A. Wacker, "Nonequilibrium Greens function theory for transport and gain properties of quantum cascade structures," *Phys. Rev.*, vol. 66, pp. 245314, 2002.
- [11] H. Callebaut, S. Kumar, B.S. Williams, Q. Hu, and J. L. Reno, "Analysis of transport properties of terahertz quantum cascade lasers," *Appl. Phys. Lett.* Vol. 83, pp. 207–209, 2003.
- [12] Y. Chassagneux, Q. J. Wang, S. P. Khanna, E. Strupiechonski, J.-R. Coudeville, E. H. Linfield, A.G. Davies, F. Capasso, M. A. Belkin, and R. " Limiting Factors to the Temperature Performance of THz Quantum Cascade Lasers Based on the Resonant-Phonon Depopulation Scheme," *IEEE J. of Quantum Electron*, vol. 2, no. 1, 2010.

- [13] C. Jirauschek, G. Scarpa, P. Lugli, M. S. Vitiello, and G. Scamarcio, "Comparative analysis of resonant phonon THz quantum cascadelasers," *J. Appl. Phys.*, vol. 101, 2007.
- [14] R. Ferreira and G. Bastard, "Evaluation of some scattering times for electrons in unbiased and biased single- and multiple-quantum-well structures," *Phys. Rev. B*, vol. 40, p. 1074, 1989.
- [15] R. F. Kazarinov and R. A. Suris, "Possibility of the amplification of electromagnetic waves in a semiconductor with a superlattice," *Soviet Phys.—Semicond.*, vol. 5, pp. 707–709, 1971.
- [16] J. H. Smet, C. G. Fonstad, and Q. Hu, "Intrawell and interwell intersubband transitions in multiple quantum wells for far-infrared sources," *J. Appl. Phys.*, vol. 79, pp. 9305–9319, 1995.
- [17] S. Kumar, Q. Hu, and J. L. Reno, "186 K operation of terahertz quantum-cascade lasers based on a diagonal design," *Appl. Phys. Lett.*, vol. 94, 2009.